

Coupling of the proton-hole and neutron-particle states in the neutron-rich ^{48}K isotope

W. Królas,¹ R. Broda,¹ B. Fornal,¹ R. V. F. Janssens,² A. Gadea,^{3,4} S. Lunardi,⁵ J. J. Valiente-Dobon,³ D. Mengoni,⁵ N. Mărginean,^{3,6} L. Corradi,³ A. M. Stefanini,³ D. Bazzacco,⁵ M. P. Carpenter,² G. De Angelis,³ E. Farnea,⁵ E. Fioretto,³ F. Galtarossa,⁵ T. Lauritsen,² G. Montagnoli,⁵ D. R. Napoli,³ R. Orlandi,³ T. Pawlat,¹ I. Pokrovskiy,³ G. Pollaro,⁷ E. Sahin,³ F. Scarlassara,⁵ D. Seweryniak,² S. Szilner,⁸ B. Szpak,¹ C. A. Ur,⁵ J. Wrzesiński,¹ and S. Zhu²

¹*H. Niewodniczański Institute of Nuclear Physics PAN, PL-31342 Kraków, Poland*

²*Physics Division, Argonne National Laboratory, Argonne, Illinois 60439, USA*

³*INFN Laboratori Nazionali di Legnaro, I-35020 Legnaro, Italy*

⁴*IFIC, CSIC-Universitat de València, E-46980 Paterna, Spain*

⁵*Dipartimento di Fisica dell'Università and INFN, I-35131 Padova, Italy*

⁶*National Institute for Physics and Nuclear Engineering, Bucharest, Romania*

⁷*Dipartimento di Fisica Teorica, Università di Torino, I-10125 Torino, Italy*

⁸*Ruder Bošković Institute, HR-10001 Zagreb, Croatia*

(Received 21 October 2011; published 1 December 2011)

Excited states in the $Z = 19$, $N = 29$ neutron-rich ^{48}K isotope have been studied using deep-inelastic transfer reactions with a thick target at Gammasphere and with a thin target at the PRISMA-CLARA spectrometer. The lowest excited states were located; they involve a proton hole in the $s_{1/2}$ or $d_{3/2}$ orbital coupled to a $p_{3/2}$ neutron. A new 7.1(5)-ns, 5^+ isomer, the analog of the $7/2^-$ isomer in ^{47}K , was identified. Based on the observed γ -decay pattern of the isomer a revised spin-parity assignment of 1^- is proposed for the ground state of ^{48}K .

DOI: [10.1103/PhysRevC.84.064301](https://doi.org/10.1103/PhysRevC.84.064301)

PACS number(s): 21.60.Cs, 23.20.Lv, 25.70.Lm, 27.40.+z

I. INTRODUCTION

The yrast and near-yrast excitations in nuclei near a closed shell are of special importance for nuclear structure since such states carry information on single-particle energies and two-body interactions. In particular, neutron-rich nuclei with nucleon numbers close to the magic ones have become a testing ground for models of exotic systems (see, e.g., Refs. [1,2]). One area of special interest concerns the isotopes around doubly-magic ^{48}Ca . While much experimental and theoretical progress has been made in the understanding of excitations involving neutrons and protons above $N = 28$ and $Z = 20$ [3–6], knowledge of structures involving proton orbitals below $Z = 20$ is more limited. This has recently led to a strong interest in the experimental investigation of the neutron-rich potassium isotopes, as they can provide guidance for the theoretical description of proton-hole states with respect to ^{48}Ca .

For the $Z = 19$, one-proton-hole potassium isotopes, the lowest excitations can be attributed to the energy-favored $s_{1/2}$ or $d_{3/2}$ proton-hole configurations. The contribution from the next available, more tightly bound $\pi d_{5/2}$ orbital is expected to be rather small. Starting with the $N = 20$, ^{39}K isotope, a dramatic change in the $\pi d_{3/2}$ and $\pi s_{1/2}$ single-particle energies occurs as the $f_{7/2}$ neutron shell is being filled in heavier odd- A isotopes. The $\pi s_{1/2}$ state decreases rapidly in energy and eventually crosses the $\pi d_{3/2}$ level at neutron number $N = 28$: see Fig. 6 and the discussion in Ref. [7]. This systematic trend is similar to that observed in the Ca isotopes and has been explained in terms of the interactions between the nucleons in the selected proton and neutron orbitals located near the Fermi surface [2]. For the $N = 29$, ^{48}K isotope, which is the subject of this paper, the predominant proton-hole excitations are coupled to the single valence neutron in the lowest available orbital, i.e., the $\nu p_{3/2}$ state.

Information on the ground state of ^{48}K was first obtained from β -decay studies of this isotope produced in a $^{48}\text{Ca}(n, p)$ reaction [8] and in high-energy fragmentation [9]. The adopted (2^-) tentative spin-parity assignment for the ground state was based on the observed pattern for the population of states in the daughter nucleus combined with arguments based on the analogy with the situation in lighter odd-odd potassium isotopes. Based on the measured $\log ft$ values for ^{48}K β decay, the Nuclear Data Sheets evaluation allows for 1^- , 2^- , or 3^- as a ground state assignment [10]. The half-life of the ^{48}K ground state was determined to be 6.8(2) s [10]. Until recently, no information on excited states of ^{48}K was available in the literature, apart from a report about the identification of an isomer [11] which will be discussed later. Some initial findings from the present study of ^{48}K were reported earlier [12] and, in a more complete way, in a conference communication [13]. On the other hand, new results on the more neutron-rich ^{49}K isotope, obtained from the data sets used here, have been published recently [7].

II. EXPERIMENTS, DATA ANALYSIS, AND RESULTS

Data from three experiments of different types were used to establish the ^{48}K level structure. In all three measurements deep-inelastic reactions with heavy ions were used to populate excited states in the isotope of interest. The first experiment, performed at the Argonne National Laboratory ATLAS accelerator, was part of a series of thick-target, γ -coincidence studies aimed at the spectroscopy of neutron-rich nuclei inaccessible in fusion-evaporation reactions [14]. The 330-MeV ^{48}Ca beam was impinging on a 50 mg/cm² thick metallic ^{238}U target placed at the center of the Gammasphere multidetector array [15]. Gamma-ray coincidence events were collected with

a trigger requiring the prompt coincidence of at least three γ rays. The beam was pulsed with a 412-ns repetition rate in order to provide a separation between prompt and delayed (isomeric and radioactive decay) events. This arrangement provides an effective means to investigate prompt events followed by an isomeric or a radioactive decay. The high-statistics coincidence data collected in this experiment have been used to establish extended level structures in several neutron-rich nuclei near the ^{48}Ca projectile (see, e.g., Refs. [5,16]), where existing data provided a means of isotopic identification. In the absence of any previous knowledge of excited states, an isotopic assignment becomes an obvious challenge for the neutron-rich potassium isotopes beyond $N = 28$. As discussed in Ref. [7], an off-beam γ -coincidence analysis revealed the presence of the known γ transitions associated with ^{48}K and ^{49}K β decays, and this observation firmly established the population of both isotopes. However, the identification of in-beam events associated with these neutron-rich K isotopes required additional information from another source.

The second experiment, aimed at providing this information, was carried out at the INFN LNL Legnaro Tandem-ALPI accelerators. The same $^{238}\text{U} + 330\text{-MeV } ^{48}\text{Ca}$ reaction was investigated with the PRISMA-CLARA spectrometer [17,18]. The wide-angle PRISMA spectrometer [17] ensured A and Z identification of the projectile-like reaction products and provided determination of the product velocity vectors, thereby allowing proper Doppler correction of the accompanying γ rays measured with the germanium detectors of the CLARA array [18]. A 0.6 mg/cm^2 ^{238}U target and a ^{48}Ca beam with a 0.6-pA average intensity were used. The PRISMA spectrometer was positioned at an angle of 52° with respect to the beam direction, i.e., in the vicinity of the calculated grazing angle of 55° . The focal plane detection system of the PRISMA spectrometer provided the required isotopic identification. The

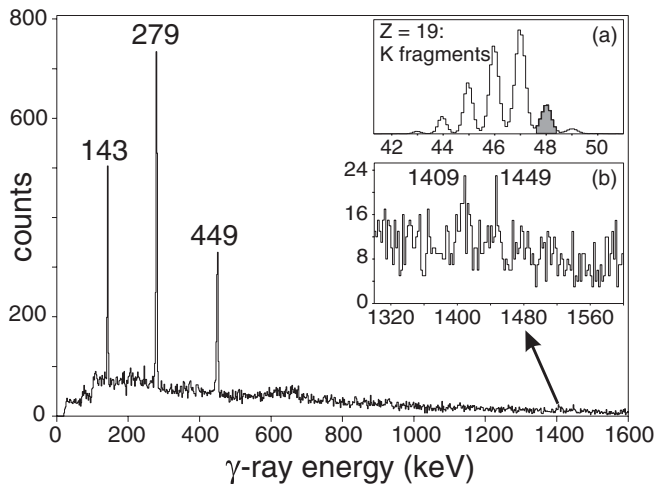


FIG. 1. Single γ -ray spectrum measured with the PRISMA-CLARA spectrometer for the ^{48}K fragments from the $^{238}\text{U} + 330\text{-MeV } ^{48}\text{Ca}$ reaction. The selection of an $A = 48$ mass window from the distribution of potassium isotopes is presented in inset (a). A high-energy portion of the spectrum, extending from 1300 to 1600 keV, showing weak 1409- and 1449-keV transitions is displayed in inset (b). See text for further discussion.

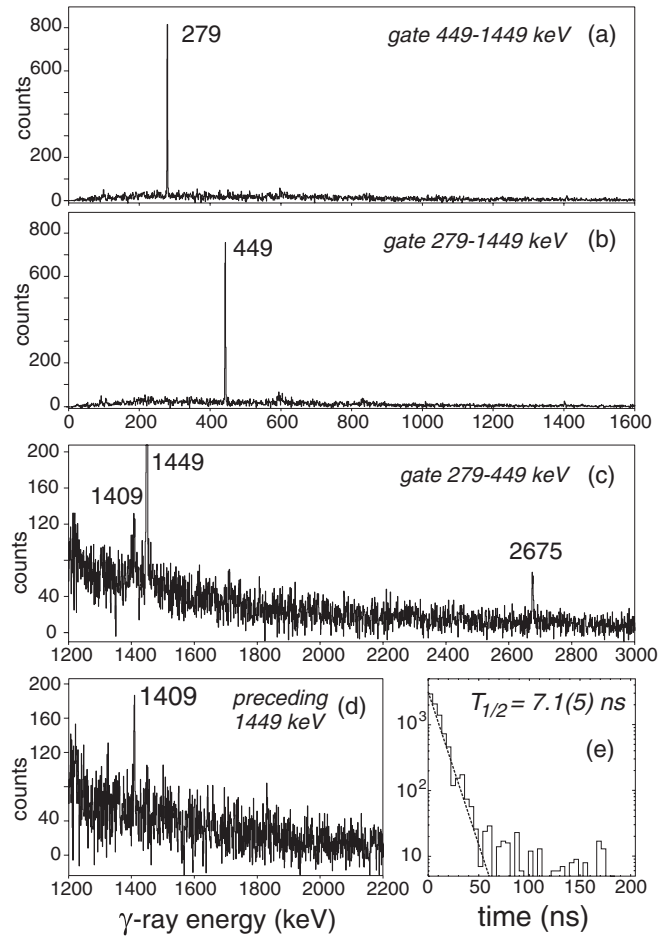


FIG. 2. Selected γ -coincidence spectra measured in the thick-target $^{238}\text{U} + 330\text{-MeV } ^{48}\text{Ca}$ experiment at Gammasphere. (a)–(c) Transitions identified in the ^{48}K isotope with various gate conditions; (d) prompt γ -ray spectrum gated by delayed 449- and 1449-keV lines; (e) decay curve of the 7.1-ns isomer obtained with gates set on the 1409–1449 and 1409–449 keV transition pairs.

γ spectra associated with several nuclei studied previously confirmed the presence of all intense transitions established in earlier thick-target experiments [19]. In addition, a few new lines appeared which correspond to transitions from short-lived states which could not be observed in thick-target measurements due to the associated large Doppler broadening.

The potassium isotope produced with the highest rate was the $N = 28$, ^{47}K isotope associated with one-proton stripping from the ^{48}Ca projectile. The yield of ^{48}K nuclei produced was $1/4$ that of ^{47}K [see Fig. 1(a)], which was nevertheless sufficient to obtain a clean spectrum of γ rays emitted by the fragments of interest. This γ spectrum is presented in Fig. 1 together with an inset (a) showing the mass window selected from the population pattern of all K isotopes as measured at the PRISMA focal plane.

The identification of three intense γ lines of 143, 279, and 449 keV in Fig. 1 allowed us to initiate the analysis of the thick-target data in order to establish coincidence relationships and construct a level scheme of ^{48}K . It was found that the 279- and 449-keV lines are in coincidence with one another as well

TABLE I. The energies and relative intensities of γ transitions identified in the ^{48}K isotope in the PRISMA-CLARA and Gammasphere $^{238}\text{U} + 330\text{-MeV } ^{48}\text{Ca}$ experiments ordered by level energy. The intensity of the 1449-keV transition established in the PRISMA-CLARA measurement is strongly reduced due to the isomeric decay. Upper intensity limits are given for the unobserved 136-, 728-, and 1898-keV linking and cross-over transitions (see text for details).

Level energy E_i (keV)	Transition energy E_γ (keV)	Relative intensities	
		PRISMA-CLARA I_γ	Gammasphere I_γ
142.7	142.7(3)	44(2)	4.3(9)
279.0	279.0(1)	100	100
	136.0		< 1.0
728.0	449.0(1)	65(2)	100
	585.0(10)		2.5(8)
	728.0		< 0.8
2177.1	1449.1(1)	3(2)	41.5(15)
	1898.0		< 0.2
	2034.5(4)		1.2(3)
3403.4	2675.4(4)		3.1(10)
3586.1	1409.0(5)	5(3)	5.4(8)

as with a third intense 1449-keV γ transition [see coincidence spectra of Figs. 2(a) and 2(b)], of which only a trace could be observed in the PRISMA-CLARA experiment [inset (b) in Fig. 1]. Moreover, coincidence events for all three transitions were found in the off-beam data. This indicated the existence of a short-lived isomer, similar to the isomer in ^{47}K which is known to decay with the 1660-keV $M2$ transition [20]. The natural assumption that the 1449-keV γ ray could correspond to an analogous $M2$ isomeric transition in ^{48}K explains the near absence of this line in Fig. 1 since nuclear products emitting γ rays with delay of a few nanoseconds are practically removed from the view of the γ detectors in the PRISMA-CLARA experiment. Consequently, in Table I, which presents the list of ^{48}K transitions, the intensities of γ lines observed in the latter experiment (column 3) represent essentially the population which excludes the isomeric branch.

Further inspection of the coincidence spectra revealed two additional weak γ lines at 1409 and 2675 keV [see Fig. 2(c)]. A sort of the data in which prompt transitions were correlated with delayed γ rays emitted within a 16–50 ns time window after the prompt events demonstrated that the 1409-keV line precedes in time the transitions identified in the decay of the isomer [see Fig. 2(d)]. This established the level with the highest excitation above the isomer observed in the present measurement as being located at 3586 keV. The observation of this low-intensity, 1409-keV γ transition above the isomer proved crucial to determine the half-life of the isomeric state from the $t_{\gamma\gamma}$ parameter. The decay curve of Fig. 2(e) corresponds to a half-life value of $T_{1/2} = 7.1(5)$ ns.

The 2675-keV line was found to be in coincidence only with the 279- and 449-keV transitions and did not exhibit any delayed component. Consequently, it was placed in the level scheme as feeding the 728-keV state from a high-energy level located at 3403 keV. The remaining 143-keV γ transition assigned to ^{48}K in the PRISMA-CLARA measurement could

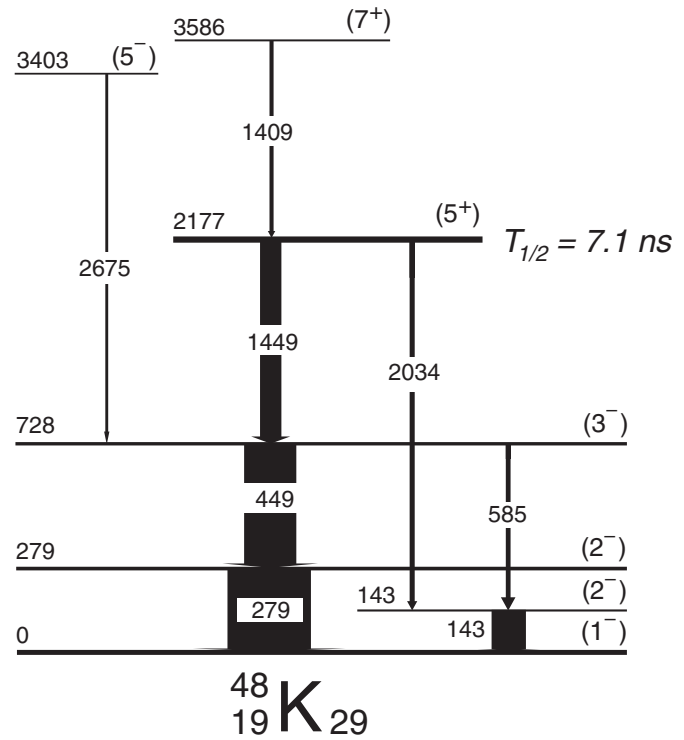


FIG. 3. The ^{48}K level scheme established in this study. See text for a discussion of the placement of the weak transitions and of the proposed spin-parity assignments.

not be readily correlated with any of the transitions discussed above in the context of the thick-target coincidence data. It was, therefore, placed as directly feeding the ground state. The proposed ^{48}K level scheme established from the observed coincidence relationships is presented in Fig. 3. The energies and intensities of the ^{48}K γ transitions determined in both experiments are listed in Table I.

To obtain additional information relevant for both the spin assignments and the interpretation of the ^{48}K levels, a further search focused on possible linking and cross-over transitions between the levels established above. In this search, the delayed- γ coincidence data selected with a narrow time window of 8–45 ns delay with respect to the beam pulse were used. These provided a much cleaner observation of the 7.1-ns isomeric decay. With this selection, the existence of a weak 585-keV γ branch feeding the 143-keV state from the 728-keV level was readily established, as is documented by the coincidence spectra of Figs. 4(a) and 4(b). On the other hand, no trace of a 728-keV cross-over transition nor of a 136-keV branch from the 279-keV to the 143-keV level could be detected. The coincidence spectrum with a single gate placed on the 1449-keV line was sufficient to extract the relative intensity for the 585-keV transition as well as to estimate upper intensity limits for the unobserved 728- and 136-keV transitions. All of the relevant values are listed in Table I.

An additional search was performed to establish the decay of the 7.1-ns isomer and compare it in detail with that of the known $7/2^-$ isomer located at 2020 keV in ^{47}K . In the

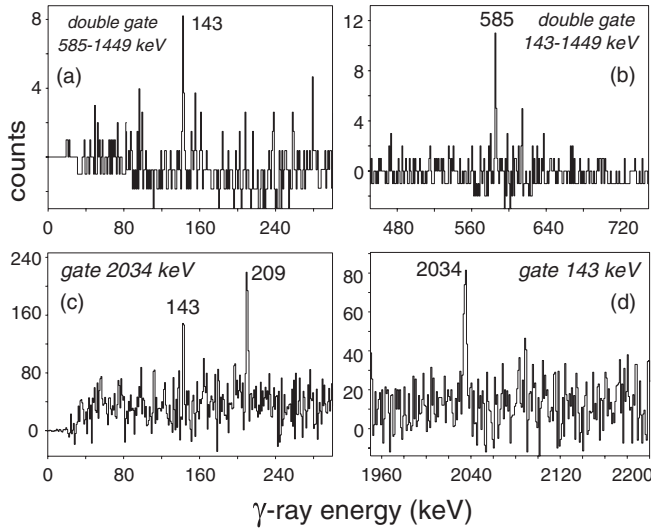


FIG. 4. Selected γ coincidence spectra measured with Gammasphere. The data were sorted with a time condition of 8–45 ns after the beam pulse in order to enhance the detection sensitivity for weak γ rays emitted in decays of nanosecond isomers. (a) and (b) Transitions identified in the 143–585–1449-keV cascade from triple $\gamma\gamma\gamma$ coincidences; (c) and (d) cascade of transitions at 143–2034 keV depopulating the ^{48}K isomer at 2177 keV. The additional 209-keV line indicated in spectrum (c) gated by the 2034-keV transition originates from the decay of the 23-ns, 8^+ isomer in ^{68}Ni [22] which was also populated in this experiment and has a line of similar energy.

latter case, a weak $E3$ branch to the $1/2^+$ ground state was observed [20] in competition with the predominant $M2$ decay to the $3/2^+$ first-excited state. The ^{47}K isomer decay is also present in the data from the Gammasphere experiment and the 2020-keV $E3$ γ branch was found to be of 5.9(12)% of the intensity of the 1660-keV $M2$ transition. This yield is more than a factor 2 smaller than the value reported in the literature [20]. The present 5.9% value was adopted for the extraction of the $B(E3)$ transition probability as the summing effects that could possibly account for the difference between the two measurements are negligible for Gammasphere detectors. A search for similar competing branches in the ^{48}K isomer decay was carried out with the double γ coincidence data in the delayed time range, since the only transition feeding the isomer (1409 keV) is by far too weak for this purpose. The γ spectrum obtained with the gate selecting the 279-keV transition did not show any trace of a 1898-keV line and a comparison with the strong 1449-keV γ ray allowed us to place a 0.5% upper intensity limit for an isomer decay branch to the 279-keV level. On the other hand, the gate set on the 143-keV transition displayed the clear presence of a 2034-keV line. This coincidence relationship was confirmed by the appearance of the 143-keV line when a reverse gate was placed on this high-energy line. Crucial segments of these coincidence spectra can be found in Figs. 4(c) and 4(d). It has to be noted that the exact energy of the 142.7-keV line fits well the energy of the first excited state as determined in the PRISMA-CLARA experiment. Also, the energy of the 2034-keV transition is in good agreement with the energy of the relevant isomer decay branch. Moreover,

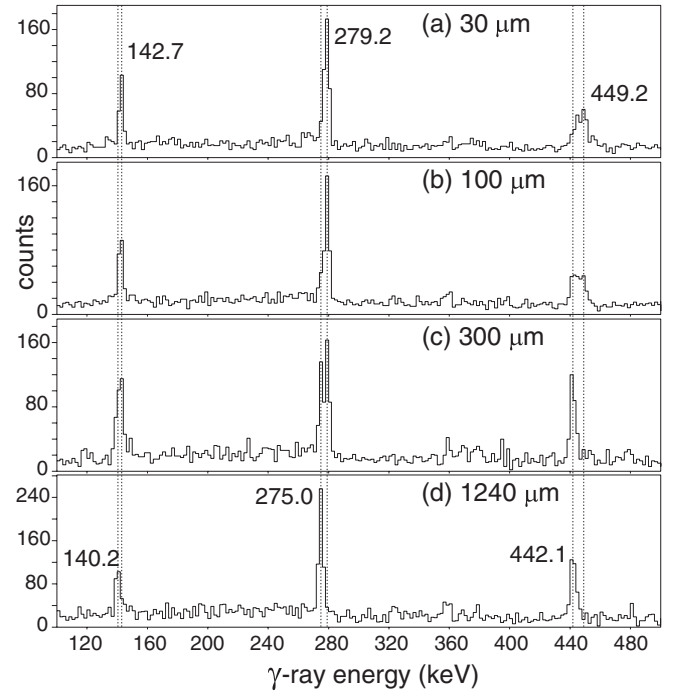


FIG. 5. The Doppler-corrected γ -ray spectra showing the 143-, 279-, and 449-keV lines at various target-degrader distances as indicated in (a)–(d). These spectra are measured in detectors located at backward angles ($\theta \sim 154^\circ$) in the array. Separation of components arising from γ emission before (shifted to low energy) and behind the degrader (properly corrected) served to derive ratios $R = I_{\text{after}}/(I_{\text{before}} + I_{\text{after}})$ used to determine lifetimes (see text and Fig. 6). The two components are indicated by dotted lines.

the high-energy 2034-keV gate provides a particularly clean coincidence spectrum, with the known ^{68}Ni 2033-keV line [21,22] being the only apparent contaminant in the gate. This accounts for the presence of the 209-keV line in the spectrum of Fig. 4(c). In summary, in the ^{48}K isomer decay, a weak decay branch to the 143-keV level was firmly established and an upper limit on the intensity of an unobserved branch to the 279-keV state was also determined. The relative intensity of the 2034-keV branch (see Table I) was obtained from the efficiency-corrected number of counts observed in the 143–2034-keV and 279–1449-keV coincidence gates. It has to be noted that the 143-keV transition intensity given in column (4) of Table I represents the summed intensity observed in the 585- and 2034-keV feeding branches and excludes the direct population of the 143-keV state seen in the PRISMA-CLARA experiment.

Whereas the proposed spin-parity assignments of states indicated in Fig. 3 will be discussed in the next section, a third experiment will now be described as it yielded additional information on the lifetimes of the ^{48}K excited states relevant for the present discussion. It is obvious that all of the ^{48}K γ transitions observed as discrete lines in the thick-target experiment are deexciting states with lifetimes and/or feeding times exceeding the ~ 1 -ps time required to stop the reaction products in the target. Apart from the 7.1-ns isomer discussed above, three other ^{48}K transitions of 143, 279, and 449 keV were sufficiently strong to measure lifetimes. For

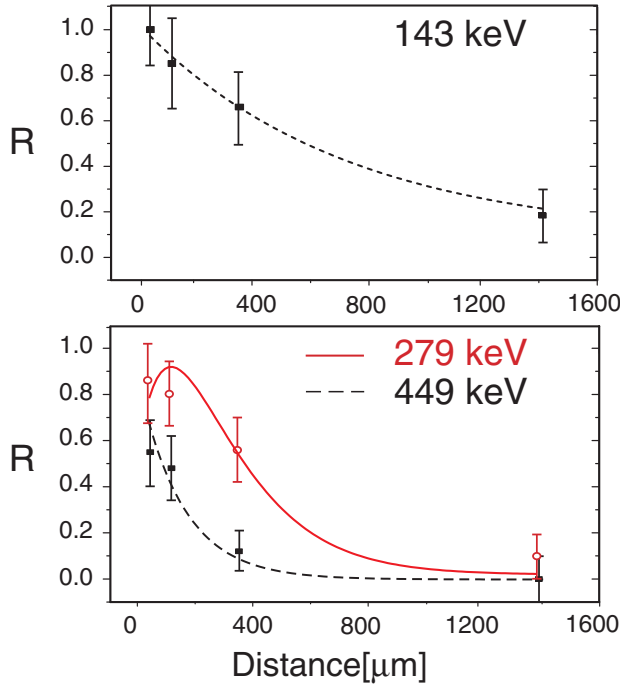


FIG. 6. (Color online) Experimental R ratios for different target-degrader distances (see text) and fits used to determine the lifetimes of the states deexcited by the 143- (top) and 279- and 449-keV (bottom) γ transitions. The feeding by the 449-keV transition is taken into account in the lifetime determination of the 279-keV state.

this purpose, the data from yet another experiment carried out with the plunger technique [23,24] at the PRISMA-CLARA spectrometer were used.

In this experiment, the 310-MeV ^{48}Ca beam was used on a 1.0 mg/cm² enriched ^{208}Pb target evaporated onto a 1.0 mg/cm² Ta support. A 4 mg/cm² natMg foil positioned at controlled distances ranging from 30 to 1240 μm after the target was used as an energy degrader of the recoiling reaction products. After passing through this degrader, the projectile-like products were selected with the magnetic spectrometer PRISMA placed at the grazing angle. The measured velocity vector allows us to correct properly for the Doppler shifts of γ rays emitted behind the degrader. Gamma-ray emission before the degrader results in a larger Doppler shift and the two components of the three transitions can be readily separated, as can be seen in Fig. 5. The relative intensities of the two observed peaks as a function of the target-degrader distance determine the lifetime of the state of interest [24].

The fits of the R ratios defined as $R = I_{\text{after}}/(I_{\text{before}} + I_{\text{after}})$ (where $I_{\text{after, before}}$ is the peak area of the transition emitted after and before the degrader) used to determine the lifetimes of the 143-, 279-, and 728-keV states are presented in Fig. 6, and the results of the lifetime analysis are listed in Table II along with the reduced transition probability values $B(M1)$ derived from the lifetimes, assuming an $M1$ multipolarity for all three transitions. The fit used in the lifetime determination of the 279-keV state takes into account the 70% feeding by the 449-keV transition from the 728-keV level. This feeding was adopted from experimental intensities and was used as a

TABLE II. Lifetimes and reduced transition probabilities established for the three strong ^{48}K γ lines measured in the experiment with the plunger by the PRISMA-CLARA spectrometer. The $B(M1)$ values were derived assuming a pure $M1$ multipolarity for the transitions. Also included is the $B(M1)$ value for the 585-keV cross-over transition and the upper limit obtained for the unobserved 136-keV transition. The lifetime and the $B(M1)$ value for the 360-keV transition in ^{47}K are listed for comparison.

Level energy E_i (keV)	Transition energy E_γ (keV)	Lifetime τ (ps)	γ branch (%)	Transition probability $B(M1)$ (W.u.)
142.7	142.7(3)	31(8)	100	0.35(9)
279.0	279.0(1)	7.7(15)	100	0.19(4)
	136.0		<1.0	< 0.016
728.0	449.0(1)	5.2(10)	97.6	0.07(1)
	585.0(10)		2.4(8)	0.0007(3)
360.0	360.0	1600(400)	100	0.0004(1)

fixed value in the lifetime fit. The error of the 279-keV state lifetime reflects both the uncertainty of the 449-keV transition lifetime and the 279-keV line fit error. A feeding correction of the 449-keV transition lifetime measurement is not necessary due to the long lifetime of the 2177-keV state, which excludes this branch from observation in the plunger experiment.

III. SPIN-PARITY ASSIGNMENTS AND DISCUSSION OF THE RESULTS

The ^{48}K isotope is one of the closest neighbors to the doubly-magic ^{48}Ca nucleus. As such it is expected to exhibit a fairly simple spectrum of excitations likely to provide valuable information on the two-body interactions of $s_{1/2}$ and $d_{3/2}$ proton holes with a single $p_{3/2}$ neutron. Moreover, as will be shown below, comparisons of shell-model expectations with the level structure of Fig. 3 and with the γ -decay information of Tables I and II provide an opportunity to propose spin and parity assignments while achieving a consistent interpretation of the observations.

For the neutron, the only configuration to consider for excitations near the ground state is the $p_{3/2}$ orbital, as the $p_{1/2}$ and $f_{5/2}$ single-particle states can be inferred to lie more than 2 MeV higher in excitation energy, based on the known structure of ^{49}Ca [25]. Similarly, from the lowest-lying states in ^{47}K [20], it can be concluded that the dominant proton configurations will be associated with $s_{1/2}$ and $d_{3/2}$ holes as the former is associated with the $1/2^+$ ground state and the latter with the $3/2^+$, 360-keV first excited state. Furthermore, the $7/2^-$ isomeric state at 2020 keV in ^{47}K has been attributed to the $\pi f_{7/2} \otimes (\pi s_{1/2}^{-2})_{0^+}$ and $\pi f_{7/2} \otimes (\pi d_{3/2}^{-2})_{0^+}$ mixed configurations [26]. It is worth noting that the same sequence of proton excitations is preserved with only small energy shifts in the presence of two additional $p_{3/2}$ neutrons in ^{49}K [7].

From these considerations it can be concluded that, below the 1-MeV excitation energy, only six states of negative parity should appear in ^{48}K : the $(1^-, 2^-)$ doublet and the

TABLE III. Comparison of the $B(M2)$ and $B(E3)$ reduced transition probabilities for transitions deexciting the $7/2^-$ isomer in ^{47}K and the 5^+ isomer in ^{48}K .

Isotope	Isomeric state			Isomeric transition			Transition probability	
	E_i (keV)	I^π	$T_{1/2}$ (ns)	E_γ (keV)	γ branch (%)	L^π	$B(M2)$ (W.u.)	$B(E3)$ (W.u.)
^{47}K	2020.0	$7/2^-$	6.3(4)	1660.0	94.4	$M2$	0.028(2)	0.60(12)
				2020.0	5.6(11)	$E3$		
^{48}K	2177.1	5^+	7.1(5)	1449.1	97.2	$M2$	0.051(4)	< 0.07
				1898.0	< 0.5	$E3$		
				2034.5	2.8(6)	$E3$		

(0^- , 1^- , 2^- , 3^-) quadruplet of states associated with the $\pi s_{1/2}^{-1} \otimes \nu p_{3/2}$ and $\pi d_{3/2}^{-1} \otimes \nu p_{3/2}$ configurations, respectively. Both states involving the $s_{1/2}$ proton hole should be expected in the low-energy spectrum. From the quadruplet of states involving the $d_{3/2}$ proton hole, however, the 2^- state should be located lowest in energy and the maximally aligned 3^- level should be pushed up significantly in energy in accordance with the well-established properties of particle-hole interactions. Another important expectation comes from the consideration that the coupling of the $p_{3/2}$ neutron to the next available $f_{7/2}$ proton (particle) should produce a quadruplet of positive-parity states with spins $I = 2$ to 5 . Here, the maximally aligned 5^+ coupling will be strongly favored to appear at the lowest energy. As a result, one would anticipate that such an yrast state would be isomeric, since the decay to the lower lying 3^- state would require a transition of $M2$ multipolarity at the minimum.

The ^{48}K level scheme established in the present work is consistent with these simple shell-model considerations. The most prominent feature in Fig. 3 is the isomeric-decay cascade of three γ transitions of 1449, 449, and 279 keV, which can be associated with the decay through the expected $5^+ \rightarrow 3^- \rightarrow 2^- \rightarrow 1^-$ sequence of states. The 2177-keV excitation energy and the 7.1-ns half-life of the isomer mirror closely the properties of the $7/2^-$ isomer in ^{47}K (located at 2020 keV and decaying with a 6.3-ns half-life by a predominant 1660-keV $M2$ transition). The $M2$ assignment of the corresponding 1449-keV transition is supported by the comparison of the extracted $B(M2)$ values for the transitions in both isotopes (see Table III). On the other hand, the measured picosecond lifetimes of the 728- and 279-keV levels strongly favor an $M1$ character for the 449- and 279-keV transitions and rule out an $E2$ multipolarity. These considerations in turn settle spin-parity assignments of $I^\pi = 3^-$ and 2^- for the 728- and 279-keV states, respectively, as well as $I^\pi = 1^-$ for the ^{48}K ground state. The low value of the upper limit of the intensity of the 728-keV cross-over transition is also consistent with these assignments and reflects the inability of the $E2$ decay branch to compete with a fast $M1$ transition within the multiplet. The proposed 1^- assignment to the ^{48}K ground state differs from the 2^- assignment proposed previously [10]. The latter could hardly be accommodated by the presently observed sequence of levels. The previously accepted 2^- assignment was based essentially on the ^{48}K β -decay pattern which was recently reanalyzed [27]. Practically no direct feeding was observed to the well-established 3^- states in the ^{48}Ca daughter

nucleus, an observation that is consistent with the present 1^- assignment.

Shell-model expectations clearly favor the $\pi d_{3/2}^{-1} \otimes \nu p_{3/2}$ configuration for the 3^- and 2^- assigned states and the $\pi s_{1/2}^{-1} \otimes \nu p_{3/2}$ one for the ground state. Whereas the remaining 0^- and 1^- states from the first quadruplet configuration could not be observed, presumably because of their unfavorable nonyrast location, the strongly populated lowest-lying 143-keV excited state is a good candidate for the 2^- member of the doublet of states involving the $s_{1/2}$ proton hole. Two experimental facts provide strong arguments in favor of this assignment and interpretation. The first is the observation of a weak 585-keV $M1$ decay branch from the 728-keV 3^- state. The associated $B(M1)$ value is about 1/100 that of the main 449-keV $M1$ branch and is very similar to that of the retarded $d_{3/2} \rightarrow s_{1/2}$ transition in ^{47}K (see Table II) [20]. The second fact, which is important since it firmly settles the 2^- assignment, is the observation of the 2034-keV $E3$ branch feeding the state directly from the 5^+ isomer. The extracted $B(E3)$ value for this branch is only about a factor 2 smaller than that obtained for the $f_{7/2} \rightarrow s_{1/2}$ $E3$ branch in ^{47}K (see Table III). On the other hand, the absence of a similar $E3$ branch to the second 2^- state at 279 keV agrees with this state involving the $d_{3/2}$ proton hole, as such a transition would require a spin flip from the $f_{7/2}$ state. Hence, it is concluded that from the two observed 2^- states, the 279-keV level is predominantly of $\pi d_{3/2}^{-1} \otimes \nu p_{3/2}$ character, while the 143-keV level structure is dominated by the $\pi s_{1/2}^{-1} \otimes \nu p_{3/2}$ configuration. The apparent negligible mixing between the two states is supported by the absence of the 136-keV $M1$ linking transition for which an upper limit of $B(M1) < 0.016$ W.u. was measured (see Table II).

Based on the simplicity of the observed ^{48}K level scheme and its straightforward interpretation derived from shell-model considerations, the present assignments can be adopted with some confidence. On the other hand, the interpretation of the two highest-lying states at 3403 and 3586 keV remains somewhat speculative. Both 2675- and 1409-keV transitions depopulating these states were observed in the thick-target data as narrow lines. Therefore, both levels must have lifetimes exceeding the 1-ps stopping time of the ^{48}K reaction products in the ^{238}U target. This finding practically excludes the presence of $M1$ transitions and makes an $E2$ assignment to both transitions likely, suggesting spin and parity $I^\pi = 7^+$

for the 3586-keV state and $I^\pi = 5^-$ for the 3403-keV level. Most naturally, the 3586-keV state can be interpreted as a 2^+ excitation of the two proton holes which are coupled as a 0^+ pair in the configuration of the 5^+ isomeric state. The 1409-keV $E2$ transition energy matches well with the 1553-keV 2^+ excitation known in ^{46}Ar [28]. On the other hand, the interpretation of the 3403-keV 5^- level can be related to the 3357-keV $f_{7/2}$ neutron-hole state seen in ^{49}Ca [19]. The energy-favored, maximally aligned spin coupling of this $f_{7/2}$ neutron hole with the $d_{3/2}$ proton hole then results in a 5^- state with the $\pi d_{3/2}^{-1} \otimes \nu f_{7/2}^{-1} p_{3/2}^2$ configuration.

The $B(M1)$ values of Table II extracted from the lifetimes of the ^{48}K states measured in the PRISMA-CLARA plunger experiment are characteristic of the fast $M1$ transitions expected between states involving the coupling of proton and neutron configurations. In this context, the fast 143-keV $M1$ ground-state transition supports the interpretation proposed above that both initial 2^- and final 1^- states are of the same configuration with a dominant $s_{1/2}$ proton hole. Somewhat contradictory to this conclusion is the large $B(M1)$ value extracted for the 279-keV transition. The latter would require a significant admixture of the $\pi d_{3/2}^{-1} \otimes \nu p_{3/2}$ configuration into the ground-state structure. It is possible that the mixing of the 1^- states involving the $s_{1/2}$ and $d_{3/2}$ proton holes is stronger than that concluded above for the 2^- levels.

The parallel study by Ishii *et al.* [11] quoted in the introduction was restricted to the isomeric decay of the ^{48}K isomer. The authors determined a longer half-life of 13(2) ns for the isomer, but the established decay pattern, although less complete, agrees in general with the present findings, including the proposed spin-parity assignments. It should be noted that the suggested presence of an unobserved Δx isomeric transition which would connect the isomeric decay cascade with the 2^- ground state reported in the literature [11] appears to be rather artificial and would add significant difficulties for the interpretation of the observed levels and their decay pattern.

Shell-model calculations involving proton-hole states in this region of nuclei are rather scarce. In the recent publication on the ^{49}K isotope [7], experimental results were compared with calculations by Nowacki and Poves [29] and Gaudefroy [30]. These unrestricted $0\hbar\omega$ shell-model calculations were carried out in the sd - pf valence space ($8 \leq Z \leq 20$, $20 \leq N \leq 40$) with the SDPF-NR and SDPF-U interactions. In this approach, protons fill the sd shells and neutrons occupy the pf orbitals. The effective interactions consist of three parts: (a) the USD interaction two-body matrix elements (TBME) for the proton-proton interaction, (b) the KB interaction TBME for the neutron-neutron interaction, and (c) the (parametrized) G -matrix interaction from Ref. [31] for the proton-neutron interaction. The monopole part of the interaction was empirically modified to provide a satisfactory description of the evolution of the effective single-particle energies across a broad region of nuclei. The SDPF-U interaction is a modified version of the SDPF-NR one and it is claimed by the authors to represent an improvement [29]. However, in Ref. [7] results using the earlier SDPF-NR interaction were selected for comparison with the full spectrum of ^{49}K experimental levels (including also the 2^+ coupling of the two $p_{3/2}$ neutrons), since only this interaction reproduced properly the $1/2^+$ spin-parity assignment of the

ground state and the presence of a $3/2^+$ level as the low-lying first excited state.

Calculations using both sets of interactions were performed for ^{48}K . In both cases, they fail to reproduce the experimental results. Both interaction sets result in a 2^- ground state, well separated from the lowest excitations. Using the SDPF-NR interaction, the first excited state is calculated to be a 1^- level at 0.42 MeV while the SDPF-U interaction predicts a second 2^- level at 0.34 MeV as the first excited state with the 1^- state located at 0.39 MeV. The agreement is somewhat better for the 3^- state observed at 728 keV: it is calculated to lie at 0.78 and 0.67 MeV using the SDPF-NR and SDPF-U interactions, respectively. However, the calculated 5^- excitation is at 2.62 and 2.97 MeV, respectively, i.e., much too low when compared to the 3403-keV energy of the proposed 5^- experimental state. In view of these disagreements, there appears to be a need to question the earlier calculations reproducing relatively well the ^{49}K isotope [7]. It is hoped that the experimental results presented here will provide further guidance for improved shell-model calculations of proton-hole excitations in the ^{48}Ca region.

IV. CONCLUSIONS

In summary, excited states which arise from the coupling of a $p_{3/2}$ neutron with $s_{1/2}$ and $d_{3/2}$ proton holes were identified in ^{48}K . A new 5^+ isomer with a half-life of $T_{1/2} = 7.1(5)$ ns, also reported in Ref. [11], corresponds to the maximally aligned coupling of the $p_{3/2}$ neutron and the $f_{7/2}$ proton. It is the analog of the $7/2^-$ isomer in ^{47}K . The observed structure of the ^{48}K excitations can be interpreted in a fairly straightforward way with considerations based on the coupling of the valence neutron with proton-hole states. The established level energies provide valuable information from which effective two-body interactions between $s_{1/2}$ and $d_{3/2}$ proton holes and the $p_{3/2}$ neutron particle can be derived. Based on the observed γ -decay pattern of the isomer and on new information from the ^{48}K β decay, a revised 1^- assignment is proposed for the ground state of ^{48}K . Two other states observed at higher excitation energy above the isomer were tentatively assigned and interpreted. It was also concluded that the presently available shell-model calculations require substantial improvements.

ACKNOWLEDGMENTS

This work was supported by the European Commission within the Sixth Framework Programme through I3-EURONS Contract No. RII3-CT2004-506065, by the US Department of Energy, Office of Nuclear Physics, under Contract No. DE-AC02-06CH11357, and by the Polish Ministry of Science and Higher Education Grants No. 1P03B05929 and No. NN202103333. A. Gadea and E. Farnea acknowledge the support of MICINN, Spain, and INFN, Italy, through the AIC10-D-000568 bilateral action. A. Gadea has been partially supported by the MICINN and Generalitat Valenciana, Spain, under Grants No. FPA2008-06419 and No. PROMETEO/2010/101.

- [1] J. Dobaczewski, N. Michel, W. Nazarewicz, M. Ploszajczak, and J. Rotureau, *Prog. Part. Nucl. Phys.* **59**, 432 (2007).
- [2] T. Otsuka, T. Suzuki, R. Fujimoto, H. Grawe, and Y. Akaishi, *Phys. Rev. Lett.* **95**, 232502 (2005), and references therein.
- [3] R. V. F. Janssens *et al.*, *Phys. Lett. B* **546**, 55 (2002).
- [4] S. N. Liddick *et al.*, *Phys. Rev. Lett.* **92**, 072502 (2004).
- [5] B. Fornal *et al.*, *Phys. Rev. C* **72**, 044315 (2005).
- [6] M. Honma, T. Otsuka, B. A. Brown, and T. Mizusaki, *Phys. Rev. C* **65**, 061301 (2002).
- [7] R. Broda *et al.*, *Phys. Rev. C* **82**, 034319 (2010).
- [8] L. G. Multhauf, K. G. Tirsell, S. Raman, and J. B. McGrory, *Phys. Lett. B* **57**, 44 (1975).
- [9] C. Detraz, D. Guillemaud, G. Huber, R. Klapisch, M. Langevin, F. Naulin, C. Thibault, L. C. Carraz, and F. Touchard, *Nucl. Phys. A* **302**, 41 (1978).
- [10] Evaluated by T. W. Burrows, *Nucl. Data Sheets* **107**, 1747 (2006).
- [11] T. Ishii, M. Asai, M. Matsuda, S. Ichikawa, A. Makishima, T. Kohno, and M. Ogawa, CNS-REP-64, 2004, p. 27.
- [12] R. Broda *et al.*, Laboratori Nazionali di Legnaro Annual Report 2006, p. 9.
- [13] W. Królas *et al.*, in *Proceedings of the Fourth International Conference on Fission and Neutron-Rich Nuclei, Sanibel Island, Florida, 2007*, edited by J. H. Hamilton, A. V. Ramayya, and H. K. Carter (World Scientific, Singapore, 2008), p. 531.
- [14] R. Broda, *J. Phys. G* **32**, R151 (2006).
- [15] I. Y. Lee, *Nucl. Phys. A* **520**, c641 (1990).
- [16] R. Broda *et al.*, *Acta Phys. Pol. B* **36**, 1343 (2005).
- [17] A. Stefanini *et al.*, *Nucl. Phys. A* **701**, 217c (2002).
- [18] A. Gadea *et al.* (EUROBALL and PRISMA-2 Collaborations), *Eur. Phys. J. A* **20**, 193 (2004).
- [19] R. Broda, *Acta Phys. Pol. B* **32**, 2577 (2001).
- [20] Evaluated by T. W. Burrows, *Nucl. Data Sheets* **108**, 923 (2007).
- [21] R. Broda *et al.*, *Phys. Rev. Lett.* **74**, 868 (1995).
- [22] T. Ishii, M. Asai, A. Makishima, I. Hossain, M. Ogawa, J. Hasegawa, M. Matsuda, and S. Ichikawa, *Phys. Rev. Lett.* **84**, 39 (2000).
- [23] J. J. Valiente-Dobon *et al.*, *Phys. Rev. Lett.* **102**, 242502 (2009).
- [24] D. Mengoni *et al.*, *Phys. Rev. C* **82**, 024308 (2010).
- [25] Evaluated by T. W. Burrows, *Nucl. Data Sheets* **76**, 191 (1995).
- [26] L. Weissman *et al.*, *Phys. Rev. C* **70**, 024304 (2004).
- [27] R. Broda (private communication).
- [28] J. Mrazek *et al.*, *Nucl. Phys. A* **734**, E65 (2004).
- [29] F. Nowacki and A. Poves, *Phys. Rev. C* **79**, 014310 (2009).
- [30] L. Gaudefroy, *Phys. Rev. C* **81**, 064329 (2010).
- [31] S. Kahana, H. C. Lee, and C. K. Scott, *Phys. Rev.* **180**, 956 (1969).